# An Optimized Motion Strategy for the Legless Capsubot Using Non-Linear Optimization

**S. Mahmoudzadeh, H. Mojallali**

*Department of Electrical Engineering, Faculty of Engineering, University of Guilan, Rasht, Iran*
*(e-mails: mahmoudzadeh@msc.guilan.ac.ir, mojallali@guilan.ac.ir)*

**Abstract:** Capsubots are miniaturized wireless capsule robots that have been recently proposed for diagnostic purposes in endoscopy. Since the capsubot needs to be swallowed by the patient, the size of the body of the capsubot is of essential importance. The size of the body is partly limited by the size of the battery, which in turn depends on the power consumption of the capsule. In this paper, a strategy is proposed that optimizes the motion of a legless capsubot and allows a large reduction in the power consumption compared to those in the literature. As a result, the size of the capsubot can potentially be reduced to a much smaller size which can be clinically more feasible. Three different profiles are defined and compared for a motion strategy and the step-time and force in each profile are optimized. Standard non-linear optimization methods are used to find the optimal motion details. Finally simulations are performed to compare the three profiles with the previously proposed motion strategies in the literature.

*Keywords:* capsubot, legless, optimization, motion strategy.

## 1. INTRODUCTION

Endoscopy is a method to study and analyze the human body orifices which was first developed in early 1800s (Spaner and Warnock, 1997). The invention of the rod-lens optical system and the fiber-optic light transmission in the mid-1900s were noteworthy advances in the history of endoscopy (Linder et al., 1997). In the past two decades, the diagnosis of most parts of the gastrointestinal (GI) track has been possible using flexible endoscope tubes. Despite the progresses made in endoscopy, the endoscope tube causes discomfort and pain for the patients, and parts of the small intestine are still inaccessible (Appleyard et al., 2000). In addition to endoscopy, there are other medical procedures such as colonoscopy and laparoscopy which are used for diagnosis of diseases in the digesting system such as colorectal cancer. Similar to endoscopy, these procedures either include invasive surgeries or exert pain to the patient′s body and often require anesthesia.

Recently, wireless capsules have been used for diagnosis and data acquisition from different parts of the GI track, for instance, in Wireless Capsule Endoscopy (WCE). Using WCE usually consists of a preparation stage before swallowing the capsule, and the main procedure takes up to 8 hours. During the procedure, the capsule moves passively through the digesting system with the peristaltic movement of the intestines, and the capsule lacks the ability to move or stop intentionally. The capsule takes a few pictures of the GI track every second, and there is possibility that it misses some points of interest (Moglia et al., 2007; Neumann et al., 2014). This problem has motivated researchers to develop capsule robots which could be remotely controlled and can actively pass through the gastrointestinal track.

Capsule robots, often called "capsubots", are mainly categorized into two groups: legged capsubots and legless capsubots. In legged capsubots, the motion mechanism is based on a set of legs or paddles that push the capsule forward (Valdastri et al., 2009; Glass et al., 2008; Zhong et al., 2015). However, legged capsubots have drawbacks such as possible pain and damage of the gastrointestinal track by the legs and fabrication difficulties. On the other hand, the motion of legless capsubot is based on the propulsion force between the capsule body and an inner mass. Fabrication simplicity makes it possible to make legless capsubots smaller than the legged ones. Also, there will be no side effects on the patient due to the capsubot traversing inside the digesting system.

The motion of a legless capsubot is pre-defined via a motion strategy. A few step-by-step motion strategies have been proposed in the literature (Liu et al., July 6-11, 2008; Lee et al., 2008; Yu et al., 2011). Others have proposed the use of off-line controllers instead of pre-defined motion strategies (Farahani et al., 2013; Mahmoudzadeh and Mojallali, 2013; Chen et al., 2009).

An important factor in the fabrication of capsubot is the size of the capsule body, because the capsule needs to be swallowed by the patient. The size of the capsule body depends on the equipment installed inside the capsubot. One of the most space consuming parts inside a capsubot is the battery (Beccani et al., 2014). A larger battery can provide more power and thus a longer operational time. However, a battery of a larger size and capacity would consume more space which is not desirable. Reducing the

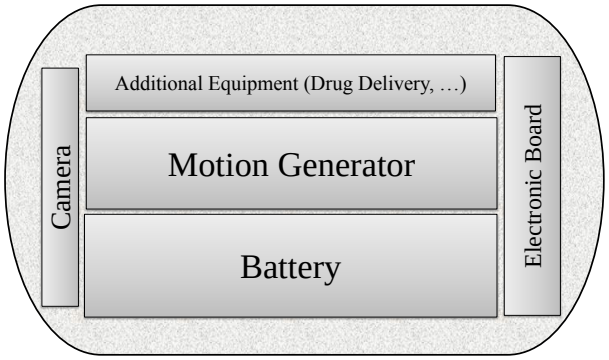


Fig. 1. A conceptual design of a legless capsubot

size of the battery, on the other hand, leads to a reduction in the size of the capsubot so that it can be swallowed more easily. From another point of view, with a smaller battery in the same size of a capsubot, the empty space can be used to fit additional components such as biopsy or drug delivery equipment.

A conceptual design of a legless capsubot is shown in Fig. 1. The capsule shell is mostly made of ABS plastic which is widely used in biomedical applications. The shell is usually fabricated using a 3D printer (Ciuti et al., 2012; Zhong et al., 2015). There are many commercially available electronic boards for controlling the capsubot. These boards meet many constraints that are required for a capsule to operate in a human body such as minimal size and operating temperature. Additional components such as a 3D accelerometer, a 3D gyroscope, pressure and temperature sensors and miniature wireless cameras can be added to the capsubot depending on the application (Beccani et al., 2014). The motion generation part of the capsubot could consist of a combination of a vibrating motor and magnets (Ciuti et al., 2010), a mechanical tail fin (Zhong et al., 2015), or other means of generating motion. In the case of this work, a linear DC motor (Huda et al., 2012) or a system containing a magnetic conductor, a magnetic conductive gasket, a coil and a magnet can be used (Chen et al., 2009).

The power consumption for the movement and thus the battery usage heavily depends on the motion strategy and the required force to move the inner mass. Therefore, optimizing the power consumption [or required force] is of critical importance. Various methods of optimization have been used in the literature in many different areas such as modeling and control of linear and nonlinear systems (Rajagopal and Ponnusamy, 2014; Rossomando, 2014). In the literature of capsubots, heuristic methods and numerical optimization methods have been the main tools used for developing a motion strategy (Yu et al., 2011; Farahani et al., 2013; Li et al., 2006). To the best of our knowledge, there has been no work that aims to minimize the power consumption of the capsubot at the design stage. In terms of power consumption, the results of the various methods in the literature do not differ significantly.

In this paper, a motion strategy is proposed that aims to minimize the power consumption of the capsubot. In order to facilitate the comparison with other methods in the literature, the maximum force is fixed and the distance that can be traveled with that limited amount of power is maximized. Alternatively, based on the proposed motion strategy, three different profiles are defined and compared and the motion is optimized using standard non-linear optimization methods to calculate the required forces and times for each step in the profile. Next, the results of the different profiles are compared and the result of the best profile is compared to the other methods in the literature. Finally, a series of simulations are held to optimize the power consumption. In order to achieve this goal, using the best profile, the maximum force is reduced and the distance covered by the capsubot is calculated. This reduction in force is continued until the speed of the capsubot is reduced to the maximum speed available in the literature. Comparing the required force to achieve the same speed for the capsubot one can find a great reduction in power consumption using the proposed mechanism in this paper.

The rest of this paper is organized as follows: In Section 2, the dynamic properties and the motion strategy of the capsubot will be described. Three force profiles for the capsubot are proposed in Section 3. Simulations will be performed in Section 4 to compare the proposed profiles and to choose the best one. Then, the results of the best profile will be compared with those of other theoretical work in the literature. Next power consumption simulations will be held. Also, sensitivity analysis will be performed to show the robustness of this profile against fabrication error. Finally, discussion and concluding remarks are presented in Section 5.

## 2. CAPSUBOT DYNAMIC PROPERTIES

A capsubot is a robot which consists of two parts: the capsule body and the inner mass. In this work, one dimensional movement is studied; that is, the inner mass can move back and forth inside the capsule body. By applying a proper force to the inner mass, the capsule body can be moved forward or backward. A schematic diagram of the capsubot and the existing forces in the capsubot system is shown in Fig. 2. For the ease of understanding, other parts of the capsubot are neglected and are considered as parts of the capsule body. As shown in Fig. 2 $x_M$ is the position of the capsule body with respect to a fixed external frame, $x_m$ is the position of the inner mass with respect to the position of capsule body, and $f_M$, $f_m$ and $U_t$ are the existing forces in the capsubot system. Also, Sliding Length is the length that the inner mass can move back and forth inside the capsule body.

In order for the capsubot to move forward, the inner mass should move in a certain cycle consisting of fast and slow steps. In this paper, a five-step motion strategy is proposed which will be described shortly. Everywhere in this paper, right/forward is the positive direction and left/backward is the negative direction. The origin point for the inner mass is the right hand side of the sliding length. The origin point for the capsule body is the starting point of the movement. In the first three steps of the proposed strategy,

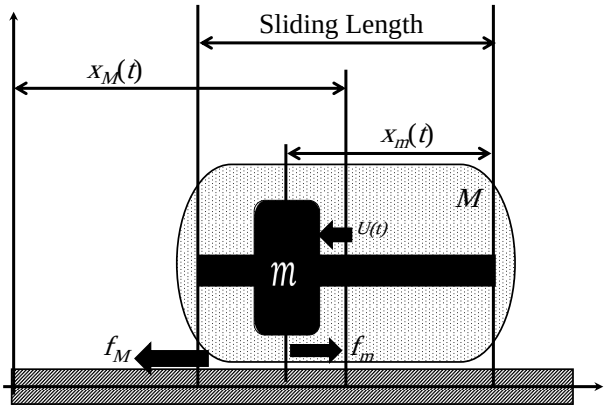


Fig. 2. Schematic diagram of the capsubot

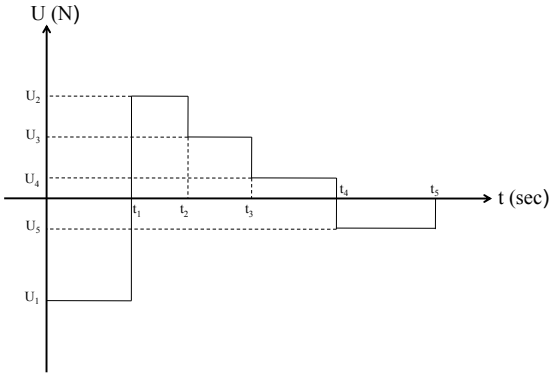


Fig. 3. Required force for the capsubot motion mechnism

the inner mass will move from the right hand side of the capsule body (sliding length) to the left hand side with a rapid lunge forcing the capsule body to move forward. The following two steps will move the inner mass to its initial place at the right hand side in a way that does not move the capsule body backward. Each of these five steps are described below:

- Step 1 ($0 \leq t \leq t_1$): In this step, a high negative force is applied to the inner mass making it accelerate and move backward. Therefore, the capsule body will move forward.
- Step 2 ($t_1 < t \leq t_2$): A positive force is applied to the inner mass reducing its speed. The speed of capsule body will decrease too.
- Step 3, ($t_2 < t \leq t_3$): A positive force equal or less than that of the previous step is applied to the inner mass to stop it at the end of the sliding length. This force should be large enough to stop the inner mass but not so large to push the capsule body backward.
- Step 4, ($t_3 < t \leq t_4$): A positive small force is applied to the inner mass to move it forward without moving the capsule body back.
- Step 5, ($t_4 < t \leq t_5$): a negative force is applied to the inner mass to stop it at its initial position.

Fig. 3 shows the required forces to satisfy the proposed strategy for the capsubot. In order to determine the amount of force and the duration of each step, the governing rules of the capsubot system at each step must be determined.

The motion mechanism is divided into two parts: the first three steps, where the inner mass is moving left and the friction force direction between the inner mass and the capsule body is to the right ($0 \leq t \leq t_3$), and the last two steps, where the inner mass is moving right and the friction force direction is to the left ($t_3 < t \leq t_5$). It should be noted that it is expected that in both parts, the capsule body is either moving forward or standing still. Applying the Newton's second law of force, the equations of acceleration for the inner mass can be calculated. The velocity and the position of the inner mass can be calculated by single and double integration of the acceleration with respect to the time, respectively. The resulting governing equations in the capsubot system are:

$$\begin{aligned} \Sigma F_m =& ma_m(t) \Rightarrow U(t) \pm f_m = ma_m(t), \\ f_m =& \mu_1 mg, \\ \Sigma F_M =& Ma_M(t) \Rightarrow U_M(t) - f_M \mp f_m = \\ & Ma_M(t), f_M = \mu_2 Mg, \end{aligned} \tag{1}$$

where $m$ is the weight of the inner mass, $M$ is the weight of the capsule body, $a_m$ is the acceleration of the inner mass, $a_M$ is the acceleration of the capsule body, $\mu_1$ is the friction coefficient between the inner mass and the capsule body, $\mu_2$ is friction coefficient between the capsule body and the outer environment, $f_m$ is the friction force between the inner mass and the capsule body, $f_M$ is the friction force between the capsule body and the environment, $g$ is the acceleration due to the gravity, and $U_M(t)$ is the force applied to the capsule body. Considering the set of equations in (1), the equation of acceleration for the inner mass will be:

$$a_m(t) = 1/m \begin{cases} U(t) + f_m & , 0 \leq t \leq t_3 \\ U(t) - f_m & , t_3 < t \leq t_5 \ . \end{cases} \tag{2}$$

It should be noted that a force equal to the fore applied to the inner mass is exerted to the capsule body in the other direction. Thus, the acceleration equation for the capsubot can be derived in order to calculate its velocity and position as follows:

$$a_M(t) = 1/M \begin{cases} U_M(t) - f_M - f_m & , 0 \leq t \leq t_3, \\ U_M(t) - f_M + f_m & , t_3 < t \leq t_5 \ . \end{cases} \tag{3}$$

In the equation above, note that $U_M(t) = -U(t)$. After calculating the equations of acceleration, velocity, and position, the values of the force and the duration of each step needs to be determined. In the next section, three force profiles will be proposed and their performance will be compared.

## 3. PROPOSED FORCE PROFILES FOR THE CAPSUBOT

In order to calculate the optimum required forces and time intervals, a few conditions need to be considered: First, the amount of force that the piezoelectric element can provide is limited to an amount of $U_{max}$. Second,

the total distance that the capsule body traverses in each cycle should be maximized and the movement should be smooth. Finally, the total time for each cycle should be minimized. These conditions are the criteria for optimizing the proposed profiles. The parameters of the capsubot used in the proposed profiles are shown in Table 1.

Table 1. Capsubot Parameters

| Parameter | Value |
|---|---|
| $M(gr)$ | 2.5 |
| $m(gr)$ | 1.5 |
| $\mu_m(N/m.sec)$ | 0.016 |
| $\mu_M(N/m.sec)$ | 0.16 |
| Sliding Length $(cm)$ | 2 |
| $U_{max}(N)$ | 0.30 |

### *3.1 Profile A*

In Profile A, it is assumed that in order to reduce the time of the first step and also maximize the capsule body traveling distance, the amount of force should be the maximum applicable force ($U_1 = -U_{max}$). The same assumption is considered for the second step to reduce the time ($U_2 = U_{max}$). In the third step, a fraction of $U_{max}$ is selected such that the stopping force for the inner mass does not make the capsule body move backward ($U_3 = U_{max}/K$). For the fourth and the fifth steps, the maximum applicable force to the inner mass which does not move the capsule body is selected. This force is equal to the friction force between the capsule body and the outer environment ($U_4 = f_M, U_5 = -f_M$). With these considerations, the acceleration equation for the inner mass and the capsule body can be written to calculate their speed and position.

$$a_m(t) = \frac{1}{m}\begin{cases} -U_{max} + f_m & , 0 \le t \le t_1 \\ U_{max} + f_m & , t_1 < t \le t_2 \\ \frac{U_{max}}{K} + f_m & , t_2 < t \le t_3 \\ f_M - f_m & , t_3 < t \le t_4 \\ -f_M - f_m & , t_4 < t \le t_5, \end{cases} \tag{4}$$

and,

$$\begin{aligned} a_M(t) =& \frac{1}{M}(U_{max} - f_M - f_m) && (5)\\ & && , 0 \le t \le t_1 \\ =& \frac{1}{M}(-U_{max} - f_M - f_m) \\ & && , t_1 < t \le t_2 \\ =& \frac{1}{M}(\frac{-U_{max}}{K} - f_M - f_m) \\ & && , t_2 < t \le t_3 \\ =& \frac{1}{M}(-2f_M + f_m) \\ & && , t_3 < t \le min\{t_s, t_4\} \\ =& 0 \\ & && , min\{t_s, t_4\} < t \le t_5, \end{aligned}$$

At time $t_3$, the capsule body might not be at a full stop. Therefore, after step 3, only the friction force $-f_M$ is applied to the capsule body until the body stops at $t_s$. After that the body will stay still until the time $t_5$. The value of $t_s$ can be calculated after determining the equations of velocity for the capsule body. Integration of (4) and (5) with respect to the time will lead to the velocity of the inner mass, $v_m$, and the capsule body, $v_M$, respectively:

$$\begin{aligned} v_m(t) =& \frac{1}{m}((-U_{max} + f_m)t) && (6)\\ & && , 0 \le t \le t_1 \\ =& \frac{1}{m}((U_{max} + f_m)(t - t_1) + v_m(t_1)) \\ & && , t_1 < t \le t_2 \\ =& \frac{1}{m}((\frac{U_{max}}{K} + f_m)(t - t_2) + v_m(t_2)) \\ & && , t_2 \le t \le t_3 \\ =& \frac{1}{m}((f_M - f_m)(t - t_3) + v_m(t_3)) \\ & && , t_3 \le t \le t_4 \\ =& \frac{1}{m}((-f_M - f_m)(t - t_4) + v_m(t_4)) \\ & && , t_4 \le t \le t_5. \end{aligned}$$

and for the capsule body:

$$\begin{aligned} v_M(t) =& \frac{1}{M}((U_{max} - f_M - f_m)t) && (7a)\\ & && , 0 \le t \le t_1 \\ =& \frac{1}{M}((-U_{max} - f_M - f_m) && (7b)\\ & (t - t_1) + v_M(t_1)) \\ & && , t_1 \le t \le t_2 \\ =& \frac{1}{M}((\frac{-U_{max}}{K} - f_M - f_m) && (7c)\\ & (t - t_2) + v_M(t_2)) \\ & && , t_2 \le t \le t_3 \\ =& \frac{1}{M}((-2f_M + f_m) && (7d)\\ & (t - t_3) + v_M(t_3)) \\ & && , t_3 \le t \le min\{t_s, t_4\} \\ =& 0 && (7e)\\ & && , min\{t_s, t_4\} \le t \le t_5. \end{aligned}$$

Note that $v_M(t_s)$ should be equal to zero. Setting (7d) equal to zero $t_s$ can be calculated:

$$\begin{aligned} 0 =& 1/M((-2f_M + f_m)(t - t_3)) + v_M(t_3) && (8)\\ \Rightarrow & t_s = t_3 + \frac{Mv_M(t_3)}{2f_M - f_m}. \end{aligned}$$

Again, with integration of the velocity with respect to the time, the positions of the inner mass and the capsule body can be calculated:

$$
\begin{aligned}
x_m(t)=&\frac{1}{m}((-U_{max}+f_m)\frac{t^2}{2}) && (9)\\
&&,0\le t\le t_1\\
=&\frac{1}{m}((U_{max}+f_m)(\frac{t^2-t_1^2}{2}-\\
&t_1(t-t_1))+v_m(t_1)(t-\\
&t_1)+x_m(t_1))\\
&&,t_1<t\le t_2\\
=&\frac{1}{m}(\frac{U_{max}+f_m}{K}(\frac{t^2-t_2^2}{2}-\\
&t_2(t-t_2))+v_m(t_2)(t-\\
&t_2)+x_m(t_2))\\
&&,t_2\le t\le t_3\\
=&\frac{1}{m}((f_M-f_m)(\frac{t^2-t_3^2}{2}-\\
&t_3(t-t_3))+v_m(t_3)(t-\\
&t_3)+x_m(t_3))\\
&&,t_3\le t\le t_4\\
=&\frac{1}{m}((-f_M-f_m)(\frac{t^2-t_4^2}{2}-\\
&t_4(t-t_4))+v_m(t_4)(t-\\
&t_4)+x_m(t_4))\\
&&,t_4\le t\le t_5,
\end{aligned}
$$

and

$$
\begin{aligned}
x_M(t)=&\frac{1}{M}((U_{max}-f_M-f_m)\frac{t^2}{2}) && (10)\\
&&,0\le t\le t_1\\
=&\frac{1}{M}((-U_{max}-f_M-f_m)\\
&(\frac{t^2-t_1^2}{2}-t_1(t-t_1))\\
&+v_M(t_1)(t-t_1)+x_M(t_1))\\
&&,t_1<t\le t_2\\
=&\frac{1}{M}((\frac{-U_{max}}{K}-f_M-f_m)\\
&(\frac{t^2-t_2^2}{2}-t_2(t-t_2))\\
&+v_M(t_2)(t-t_2)+x_M(t_3))\\
&&,t_2\le t\le t_3\\
=&\frac{1}{M}((-2f_M+f_m)\\
&(\frac{t^2-t_3^2}{2}-t_3(t-t_3)\\
&+v_M(t_3)(t-t_3)+x_M(t_3))\\
&&,t_3\le t\le min\{t_s,t_4\}\\
=&\frac{1}{M}(x_M(min\{t_s,t_4\}))\\
&&,min\{t_s,t_4\}\le t\le t_5.
\end{aligned}
$$

After finding the position of the inner mass and the capsule body, Profile A is completed. Profile B is presented in the next subsection.

### *3.2 Profile B*

In order to overcome a possible step back in the motion of the capsubot the author suggests to change the forces in the second step of Profile A. Both amounts of the forces in the second and third steps are assumed to be a fractions of the maximum applicable force to the inner mass. In other words $U_2 = U_{max}/K_1$ and $U_3 = U_{max}/K_2$. Considering these new assumptions for the force profile, the equations of acceleration for the inner mass and the capsule body can be obtained:

$$
a_m(t) = 1/m\begin{cases}
-U_{max}+f_m & ,0\le t\le t_1\\
\frac{U_{max}}{K_1}+f_m & ,t_1<t\le t_2\\
\frac{U_{max}}{K_2}+f_m & ,t_2<t\le t_3\\
f_M-f_m & ,t_3<t\le t_4\\
-f_M-f_m & ,t_4<t\le t_5\ ,
\end{cases} \qquad (11)
$$

and

$$
\begin{aligned}
a_M(t)=&\frac{1}{M}(U_{max}-f_M-f_m) && (12)\\
&&,0\le t\le t_1\\
=&\frac{1}{M}(\frac{-U_{max}}{K_1}-f_M-f_m)\\
&&,t_1<t\le t_2\\
=&\frac{1}{M}(\frac{U_{max}}{K_2}-f_M-f_m)\\
&&,t_2<t\le t_3\\
=&\frac{1}{M}(-2f_M+f_m)\\
&&,t_3<t\le min\{t_s,t_4\}\\
=&0\\
&&,min\{t_s,t_4\}<t\le t_5.
\end{aligned}
$$

The same calculations as those in the subsection 3.1 should be performed to determine the equations for the velocity and the position of the inner mass and the capsule body in Profile B.

### *3.3 Profile C*

In the force profile C it is assumed that in the first and second steps the forces are fractions of the maximum applicable force ($U_1 = -U_{max}/K_1, U_2 = U_{max}/K_2$). In the third step the force is selected twice the friction force between capsule body and outer environment ($U_3 = 2f_M$). This selection was made such that in the third step, the high stopping force for the inner mass does not make the capsule body move backward. The amount of force for the fourth step is selected equal to $f_M$ as in previous profiles. An important change was made in the fifth step: In this step the amount of force was chosen as the maximum amount of force that the piezoelectric element could produce ($U_5 = -U_{max}$). This selection will stop the inner mass in a shorter time. It will also move the capsule body forward similar to the first step. Therefore, at the start of next cycle the capsule body will have an initial speed and moves faster. For the ease of calculation and also having a smooth movement the amount of force in the fifth step is select equal to the amount of force in the first step ($U_5 = -U_{max}/K_1$). The acceleration equations for the capsubot system are:

$$a_m(t) = 1/m \begin{cases} \frac{-U_{max}}{K_1} + f_m & , 0 \le t \le t_1 \\ \frac{U_{max}}{K_2} + f_m & , t_1 < t \le t_2 \\ 2f_M + f_m & , t_2 < t \le t_3 \\ f_M - f_M & , t_3 < t \le t_4 \\ \frac{-U_{max}}{K_1} - f_m & , t_4 < t \le t_5 \ , \end{cases} \quad (13)$$

and

$$\begin{aligned} a_M(t) = & \frac{1}{M}(\frac{U_{max}}{K_1} - f_M - f_m) \quad (14) \\ & , 0 \le t \le t_1 \\ = & \frac{1}{M}(\frac{-U_{max}}{K_2} - f_M - f_m) \\ & , t_1 < t \le t_2 \\ = & \frac{1}{M}(-3f_M - f_m) \\ & , t_2 < t \le t_3 \\ = & \frac{1}{M}(-2f_M + f_m) \\ & , t_3 < t \le min\{t_s, t_4\} \\ = & 0 \\ & , min\{t_s, t_4\} < t \le t_4 \\ = & \frac{1}{M}(\frac{U_{max}}{K_1} - f_M + f_m) \\ & , t_4 < t \le t_5. \end{aligned}$$

It should be noted that in (14) if the capsule body doesn't stop before the time $t_4$ ($t_4 \le t_s$) the time interval $min\{t_s, t_4\} < t \le t_4$ would be empty. With resolving all the equations of proposed profiles, in the next Section, they will be optimized to achieve the optimum time duration and amount of forces for each step in the proposed profiles.

## 4. SIMULATION AND RESULT

In this section the proposed profiles in the previous Section are optimized and compared with each other. The results of the best profile will be compared with results of other work in the literature. Next, a sensitivity analysis will be performed to show the robustness of the best of the proposed profiles.

### *4.1 Optimization*

After calculating the governing equations of the capsubot in each profile, considering the criteria mentioned before, the profile can be optimized to determine $t_1$ through $t_5$. These criteria and the maximization problem can be described as the below optimization problem:

maximize

$$x_M(t_5),$$

subject to

$$\begin{aligned} & x_m(t_3) = \text{sliding length}, \\ & x_m(t_5) = 0, \\ & v_m(t_3) = 0, \\ & v_m(t_5) = 0. \end{aligned}$$

Using the non-linear optimization toolbox in MATLAB, the problem was optimized and the results for the duration of each step and the value of $K$ for Profile A are shown in Table 2. The results for the trajectories of the inner mass and the capsule body are shown in Fig. 4. It can be seen that the required criteria for the capsubot are almost satisfied. Although a minor step back can be seen at the end of step three, but the capsule is moving forward and the inner mass is oscillating in the sliding length of the capsule body as expected.

Table 2. The values of the parameters in Profile A

| Parameter | Value |
|---|---|
| $t_1(msec)$ | 6.5 |
| $t_2(msec)$ | 12.6 |
| $t_3(msec)$ | 13.1 |
| $t_4(msec)$ | 95.7 |
| $t_5(msec)$ | 178.3 |
| $K$ | 1 |

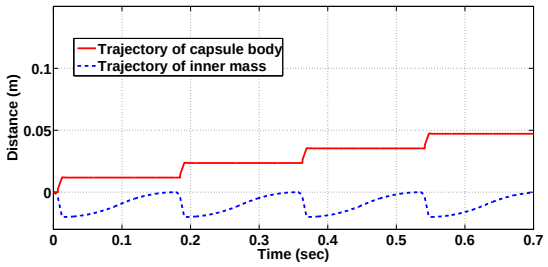


Fig. 4. Capsubot trajectory in Profile A

Table 3. The values of the parameters in Profile B

| Parameter | Value |
|---|---|
| $t_1(msec)$ | 10.0 |
| $t_2(msec)$ | 19.4 |
| $t_3(msec)$ | 24.2 |
| $t_4(msec)$ | 91.1 |
| $t_5(msec)$ | 157.7 |
| $K_1$ | 1 |
| $K_2$ | 10 |

Performing the same optimization process for Profile B as it was done for Profile A, the problem was optimized. The results for the step times, $K_1$, and $K_2$ are shown in Table 3. The trajectories of the capsubot body and the inner mass are illustrated in Fig. 5. As it is shown in Table 3 $K_1 = 1$ and $K_2 = 10$ which are the least and the most values in their defined range in the program. The value of $K_1$ shows that in order to minimize the total cycle time, the amount of force in the second step is maximized. Also, in the third step the force is minimized to prevent backward movement of the capsule body. Although the value of force in the third step is far less than the second and first steps, but there is still a considerable step back seen in the third step of moving of the capsule body.

In Profile C, the optimized values for the times and coefficients of $K_1$ and $K_2$ are shown in Table 4. As it can be seen in Table 4 the values of $K_1$ and $K_2$ are almost equal to unit. These values show that in order to reduce

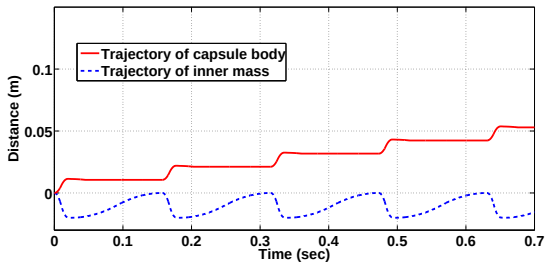


Fig. 5. Capsubot trajectory in Profile B

Table 4. The values of the parameters in Profile C

| Parameter | Value |
|---|---|
| $t_1(msec)$ | 10.0 |
| $t_2(msec)$ | 19.9 |
| $t_3(msec)$ | 20.4 |
| $t_4(msec)$ | 147.2 |
| $t_5(msec)$ | 148.7 |
| $K_1$ | 1.000 |
| $K_2$ | 1.003 |

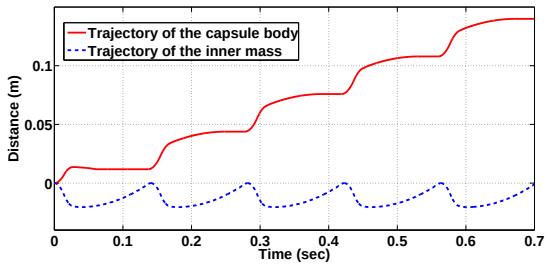


Fig. 6. Capsubot trajectory in Profile C

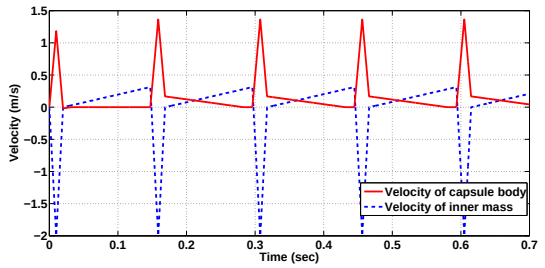


Fig. 7. Capsubot velocity in Profile C

the travel time in the first three steps the amount of force should be maximized. It should be noted that despite of the reduction in the force of third step, the total time of the cycle is still less than the previous profiles. The trajectory of capsubot, its velocity and the applied force to the inner mass for Profile C are illustrated in Figs. 6 through 8.

In Fig. 6 significant improvement has been made in Profile C compared to Profile A and Profile B. There is no step back in the trajectory of capsubot. And, it traverse almost twice as the previous profiles.

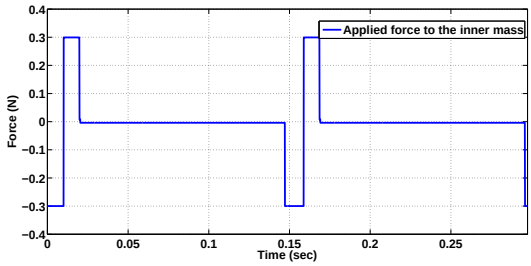


Fig. 8. Applied for to the inner mass in Profile C

Table 5. Capsubot parameters in (Lee et al., 2008)

| Parameter | $m$ | $M$ | $\mu_1$ | $\mu_2$ | $SL$ | $U_{max}$ |
|---|---|---|---|---|---|---|
| Value | 3 gr | 4 gr | 0 | 0.3 | 2 cm | 0.3 N |

Table 6. Comparing results with (Lee et al., 2008) and (Yu et al., 2011)

| Case | Est. cycle time (sec) | Est. distance traversed (cm) | Speed (cm/sec) |
|---|---|---|---|
| **This work** | 0.13 | 2.4 | 18.14 |
| **(Lee et al., 2008)-1** | 0.21 | 1.1 | 5.24 |
| **(Lee et al., 2008)-2** | 0.23 | 2.2 | 9.57 |
| **(Lee et al., 2008)-3** | 0.18 | 1.1 | 6.11 |
| **(Yu et al., 2011)** | 0.18 | 1.4 | 7.78 |

Table 7. Capsubot parameters in (Mahmoudzadeh and Mojallali, 2013)

| Parameter | $m$ | $M$ | $\mu_1$ | $\mu_2$ | $SL$ |
|---|---|---|---|---|---|
| Value | 3 gr | 4 gr | 0 | 0.1 | 5 cm |

### *4.2 Comparing with other work*

Some of the other work in the literature with parameters of capsubot close to this work are selected to be compared with the results of Profile C. Lee et al. (2008) proposed three different methods for the motion strategy of capsubot. Also, Yu et al. (2011) has presented an acceleration profile. The parameters of capsubot which were used in these work are shown in Table 5. In Table 5, SL is the sliding length of the capsubot. The capsubot system was optimized with Profile C for these parameters. The results for an estimated total time and the distance that the capsule body travels in the second iteration of all the methods are shown in Table 6.

Table 6 shows that the proposed motion strategy has significant improvement compared to the other methods. The capsule body moves up to 5 times faster compared to the other methods. Gaining high speed is not the only aim of designing a motion profile for the capsubot system. Nevertheless, achieving higher speed for the capsubot with the same amount of power consumption is equivalent to achieving the same speed with lower power consumption. This is a critical criterion in miniaturizing the capsubot system and making it easier to swallow for the patient. Fig. 9 compares the result of this work with that of (Mahmoudzadeh and Mojallali, 2013) under the same optimization parameters. These parameters are shown in Table 7.

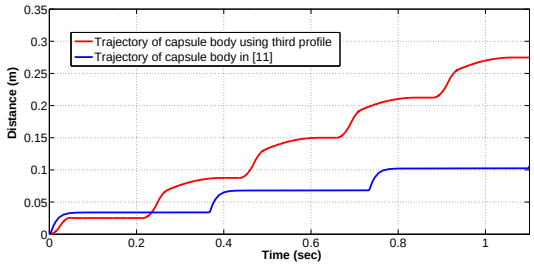


Fig. 9. Comparing result with (Mahmoudzadeh and Mojallali, 2013)

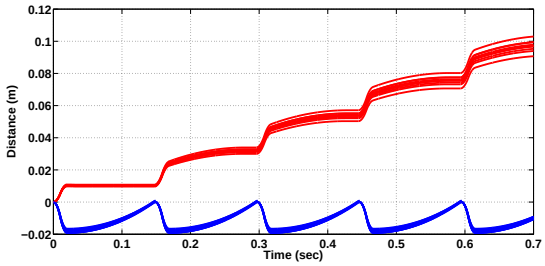


Fig. 10. Trajectory of capsubot for the corrupted cases

It can be seen in Fig. 9 that the capsubot moves a slightly shorter distance in the first cycle. In contrast, in the following cycles, the proposed method generates a longer travel distance and a much shorter total cycle time.

### *4.3 Power Consumption Optimization*

In Section 4.2, we saw that Profile C has a better performance than those in the literature. In this section, we aim to reduce the maximum force used to move the inner mass and calculate the distance that the capsule traverses, the cycle time and the speed of the capsubot. This reduction is continued until the speed of the capsubot reaches the maximum speed in the literature previously shown in Table 6. The reduction in the maximum required force to move the inner mass means lower power consumption which in turn leads to a smaller battery and a smaller piezoelectric element. Hence, the capsubot can be manufactured in a smaller size or other equipment can be installed in the capsubot. The results for different values of maximum force and corresponding distance, cycle time and capsule speed are shown in Table 8. It should be noted that the parameters of the capsubot are the same parameters used in section 4.2.

Table 8. Reducing the maximum force to optimize power consumption and achieve the desired speed

| Max. Force (N) | Distance (cm) | Cycle Time (sec) | Speed (cm/sec) |
|---|---|---|---|
| 0.3 | 2.41 | 0.13 | 18.14 |
| 0.2 | 2.34 | 0.14 | 16.65 |
| 0.1 | 2.08 | 0.16 | 13.21 |
| 0.09 | 2.02 | 0.16 | 12.59 |
| 0.08 | 1.94 | 0.16 | 11.86 |
| 0.07 | 1.85 | 0.17 | 10.99 |
| 0.06 | 1.73 | 0.17 | 9.95 |
| 0.055 | 1.66 | 0.18 | 9.35 |
| 0.05 | 1.57 | 0.18 | 8.68 |

Table 8 shows that, using an approximate force of 0.055 $(N)$ as the maximum force, the speed of capsubot reaches 9.35 $(cm/sec)$. This amount of force is one sixth of the maximum force used in (Lee et al., 2008).

### *4.4 Sensitivity Analysis*

In all of the proposed profiles, all the settings for the capsubot such as initial values and values boundaries were determined for the parameters of the capsubot which are shown in Table 1. But in the real world application one cannot guaranty to fabricate the whole capsubot system with those exact values and some error should be considered. In order to show the robustness of the proposed method to the fabrication error, the parameters of the capsubot were changed randomly. A maximum error of $\pm 5\%$ of the original values of sliding length, $U_{max}$, $\mu_1$, $\mu_2$, the weight of capsule body, and the weight of the inner mass were added to these parameters randomly. After changing the parameters of the capsubot for 10 random different cases, the output of the capsubot was calculated. The step times used for sensitivity analysis are the times in Profile C. Table 9 shows the corruption percentages for the parameters and the distance that the capsule body traversed in the second iteration of each case in centimeter. Fig. 10 illustrates the trajectory of the capsubot body and the inner mass for these cases.

As is it shown in Fig. 10, minor and acceptable errors in the fabrication of the capsubot will not affect the proposed profile and the capsule system still performs as expected. It is suggested to consider an extra margin for the sliding length to avoid collision in cases that the error makes the inner mass to move back and forth a slightly longer distance than the expected value.

## 5. CONCLUSIONS AND FUTURE RESEARCH DIRECTIONS

In this paper, a novel motion strategy for capsubots was proposed. Based on this motion strategy, three different profiles were presented. All the proposed profiles were optimized using non-linear optimization methods. The best profile was chosen based on different criteria such as the distance covered in one cycle, total cycle time, and the smoothness of movement. The result of the trajectory of the capsubot for the best profile was compared with those in the literature. The results showed significant improvement in the efficiency of the capsubot based on the speed, the cycle time and the traversing distance proposed in this work. Power consumption optimization was performed and as a result, a large reduction in the power consumption was obtained. Finally, sensitivity analysis was performed, and the robustness of the proposed mechanism against fabrication error was shown. Future work includes using other methods of optimization such as heuristic methods, adding specialized criteria to the optimization problem to achieve additional desired characteristic of the capsubot, and fabrication of such a capsubot and evaluation of the proposed profiles for the capsubot system in real world application.

Table 9. Corruption percentages in the values of the parameters and the capsule body traveling distance

| Case | $U_{max}$ | $SL$ | $\mu_1$ | $\mu_2$ | $M$ | $m$ | $x_M(t_5)$ |
|---|---|---|---|---|---|---|---|
| 1 | 1.82% | -4.4% | -4.6% | -4.3% | 0.2% | -4.0% | 2.55 |
| 2 | 3.2% | 3.2% | 2.2% | -3.5% | 1.6% | 0.2% | 2.63 |
| 3 | 1.5% | 4.7% | 3.0% | -0.5% | -0.7% | 3.3% | 2.70 |
| 4 | -3.7% | -4.2% | -3.3% | -1.1% | 3.3% | 3.0% | 2.47 |
| 5 | -1.0% | -4.4% | 0.3% | -0.8% | 1.7% | 1.3% | 2.40 |
| 6 | -07% | -2.1% | -4.8% | 4.8% | -3.3% | -3.9% | 1.46 |
| 7 | -3.0% | -1.3% | -0.1% | -1.6% | 4.5% | 4.2% | 2.24 |
| 8 | 2.4% | -4.5% | -2.3% | -0.8% | 0.5% | 4.4% | 2.31 |
| 9 | 4.9% | -0.8% | -2.0% | 2.0% | 1.7% | 0.4% | 2.44 |
| 10 | 1.7% | 2.0% | -3.2% | -3.8% | 5.0% | -3.3% | 2.39 |

## REFERENCES


Appleyard, M., Fireman, Z., Glukhovsky, A., Jacob, H., Shreiver, R., Kadirkamanathan, S., Lavy, A., Lewkowicz, S., Scapa, E., Shofti, R., et al. (2000). A randomized trial comparing wireless capsule endoscopy with push enteroscopy for the detection of small-bowel lesions. *Gastroenterology*, 119(6), 1431–1438.

Beccani, M., Susilo, E., Di Natali, C., and Valdastri, P. (2014). Smac–a modular open source architecture for medical capsule robots. *Int J Adv Robot Syst*, 11, 188.

Chen, W., Fang, M., and Yu, H. (2009). Model predictive control applied into time delay capsubot system. In *Intelligent Human-Machine Systems and Cybernetics, 2009. IHMSC'09. International Conference on*, volume 1, 112–115. IEEE.

Ciuti, G., Pateromichelakis, N., Sfakiotakis, M., Valdastri, P., Menciassi, A., Tsakiris, D., and Dario, P. (2012). A wireless module for vibratory motor control and inertial sensing in capsule endoscopy. *Sensors and Actuators A: Physical*, 186, 270–276.

Ciuti, G., Valdastri, P., Menciassi, A., and Dario, P. (2010). Robotic magnetic steering and locomotion of capsule endoscope for diagnostic and surgical endoluminal procedures. *Robotica*, 28(2), 199.

Farahani, A.A., Suratgar, A.A., and Talebi, H.A. (2013). Optimal controller design of legless piezo capsubot movement. *International Journal of Advanced Robotic Systems*, 10, 1–7.

Glass, P., Cheung, E., and Sitti, M. (2008). A legged anchoring mechanism for capsule endoscopes using micropatterned adhesives. *Biomedical Engineering, IEEE Transactions on*, 55(12), 2759–2767.

Huda, M.N., Yu, H., and Goodwin, M.J. (2012). Experimental study of a capsubot for two dimensional movements. In *Control (CONTROL), 2012 UKACC International Conference on*, 108–113. IEEE.

Lee, N., Kamamichi, N., Li, H., and Furuta, K. (2008). Control system design and experimental verification of capsubot. In *Intelligent Robots and Systems, 2008. IROS 2008. IEEE/RSJ International Conference on*, 1927–1932. IEEE.

Li, H., Furuta, K., and Chernousko, F. (2006). Motion generation of the capsubot using internal force and static friction. In *Decision and Control, 2006 45th IEEE Conference on*, 6575–6580. IEEE.

Linder, T.E., Simmen, D., and Stool, S.E. (1997). Revolutionary inventions in the 20th century: the history of endoscopy. *Archives of OtolaryngologyHead & Neck Surgery*, 123(11), 1161.

Liu, Y., Yu, H., and Yang, T. (July 6-11, 2008). Analysis and control of a capsubot. In *Proceedings of the 17th World Congress, The International Federation of Automatic Control Seoul, Korea*, 756–761.

Mahmoudzadeh, S. and Mojallali, H. (2013). An optimized pid for legless capsubots using modified imperialist competitive algorithm. In *Robotics and Mechatronics (ICRoM), 2013 First RSI/ISM International Conference on*, 194–199. IEEE.

Moglia, A., Menciassi, A., Schurr, M.O., and Dario, P. (2007). Wireless capsule endoscopy: from diagnostic devices to multipurpose robotic systems. *Biomedical Microdevices*, 9(2), 235–243.

Neumann, H., Fry, L.C., Nägel, A., and Neurath, M.F. (2014). Wireless capsule endoscopy of the small intestine: a review with future directions. *Current opinion in gastroenterology*, 30(5), 463–471.

Rajagopal, K. and Ponnusamy, L. (2014). Biogeography-based optimization of pid tuning parameters for the vibration control of active suspension system. *Journal of Control Engineering and Applied Informatics*, 16(1), 31–39.

Rossomando, F.G. (2014). Sliding mode control for trajectory tracking of a non-holonomic mobile robot using adaptive neural networks. *Journal of Control Engineering and Applied Informatics*, 16(1), 12–21.

Spaner, S.J. and Warnock, G.L. (1997). A brief history of endoscopy, laparoscopy, and laparoscopic surgery. *Journal of Laparoendoscopic & Advanced Surgical Techniques*, 7(6), 369–373.

Valdastri, P., Webster, R., Quaglia, C., Quirini, M., Menciassi, A., and Dario, P. (2009). A new mechanism for mesoscale legged locomotion in compliant tubular environments. *Robotics, IEEE Transactions on*, 25(5), 1047–1057.

Yu, H., Huda, M.N., and Wane, S.O. (2011). A novel acceleration profile for the motion control of capsubots. In *Robotics and Automation (ICRA), 2011 IEEE International Conference on*, 2437–2442. IEEE.

Zhong, Y., Du, R., and Chiu, P.W. (2015). Tadpole endoscope: a wireless micro robot fish for examining the entire gastrointestinal (gi) tract. *HKIE Transactions*, 1–6.